IEEE Access
Multidisciplinary | Rapid Review | Open Access Journal

Received October 2, 2019, accepted October 22, 2019, date of publication November 4, 2019, date of current version November 14, 2019.

Digital Object Identifier 10.1109/ACCESS.2019.2950983

Blackbox Polytopic Model With Dynamic Weighting Functions for DC-DC Converters

AIRÁN FRANCÉS, (Member, IEEE), RAFAEL ASENSI, AND JAVIER UCEDA, (Fellow, IEEE)
Centro de Electronica Industrial (CEI), Universidad Politécnica de Madrid, 28040 Madrid, Spain

Corresponding author: Airán Francés (airan.frances@upm.es)

This work was supported by the Spanish Ministry of Economy and Competitiveness under the Project IDENMRED under Grant DPI2016-78644-P.

ABSTRACT DC electric power distribution is becoming popular due to the proliferation of renewable sources and storage elements in applications such as electric vehicles, ships, aircrafts, microgrids, etc. These systems are characterized by a high integration of power electronic converters. From a system-level perspective, it would be desirable to design this kind of systems using commercial-off-the shelf converters. However, in general, the manufacturers do not provide a behavioral model of the devices in order to analyze the dynamic behavior of the interconnected system before the actual implementation. In the literature, several blackbox modeling techniques have been proposed to overcome this lack of information. This paper proposes the integration of dynamic weighting functions to the polytopic model in order to improve the accuracy of the behavioral models when the input variables change sharply. A boost converter is used as case study and the performance of the proposed model is compared with the most relevant techniques that can be found in the literature.

INDEX TERMS Blackbox models, dc microgrids, dc-dc converters, dynamic interactions, electronic power distribution, modeling, system identification, nonlinear models.

I. INTRODUCTION

Power Electronic Converters (PEC) are an enabling technology in the integration of distributed energy sources and storage elements in Electric Power Distribution Systems (EPDS). In traditional EPDS the dynamic is imposed by slow rotating synchronous generators and it is coupled with the distribution and consumption stages. The energy distribution is ensured by means of redundancy and oversized designs. PECs provide dynamic decoupling and controllability, allowing improvements in the reliability, efficiency, and cost of the whole system [1]. Furthermore, PECs enable dc power distribution through dc microgrids, which are the context of this work. The same conclusions can be extrapolated to other EPDS such as those used in electric vehicles, data centers, etc.

The dynamic decoupling capability of the PECs has encouraged the use of a hierarchical structure in the EPDS [2]. In this structure the system consists of autonomous subsystems, named nano/microgrids, which can work in grid-connected or in islanded modes. An important advantage of this approach is that the overall complexity is reduced, as each microgrid is in charge of controlling their own generation, storage and consumption elements. The connection to the rest of the system is performed through a PEC, which is considered as the Point of Common Coupling (PCC) converter (Fig. 1).

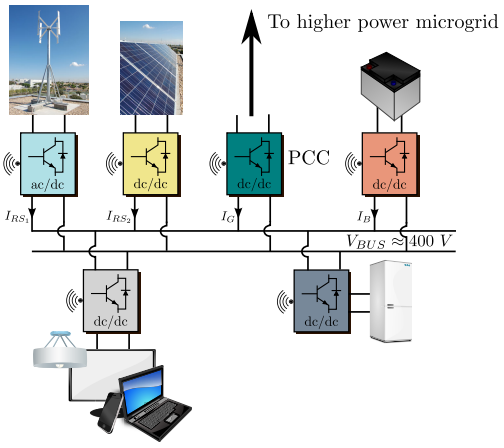

FIGURE 1. DC microgrid scheme of a residential building.

The associate editor coordinating the review of this manuscript and approving it for publication was Sanjeevikumar Padmanaban.

The PCC converter is in charge of the connection and disconnection from the rest of the systems and the power exchange. Besides, due to its dynamic decoupling capability, the microgrid can be considered as a single load, which highly simplifies the design of the upstream system. Similarly, several microgrids can be connected together creating a higher power microgrid, and so on, (Fig. 2).

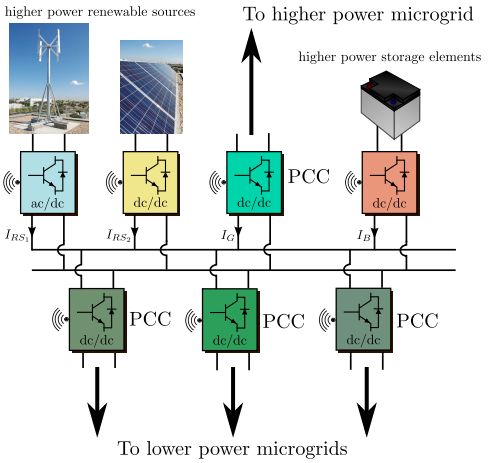

FIGURE 2. DC microgrid scheme of a group of residential buildings.

The integration of PECs in the EPDS provide a huge amount possibilities, but it also comes with a price. One of the most challenging aspects about PEC-based EPDS is the dynamic interaction among the converters. Commercial-Off-The-Shelf (COTS) converters are designed individually to have a specific dynamic response, however, when several COTS converters are connected together, their dynamic responses will be coupled and the response of the interconnected system will not be as expected. This effect can impact on the power quality of the system or even destabilize it.

In addition to this, the microgrids are characterized by having a wide range of operating conditions due to the variability of the power delivered by the renewable sources, the state of charge of the batteries, the changing power consumption, and the presence or not of the grid. In general, the wide range of operating conditions of the PECs compromises the assumptions necessary to apply small-signal approximations in order to make dynamic or stability analyzes. The PECs are nonlinear elements due to their switching nature. This nonlinearity is reflected in their static and dynamic response, which depends on the operating point. Consequently, the possibility of obtaining accurate behavioral models of COTS converters is very interesting in this kind of applications.

Different models have been proposed in order to perform dynamic and stability analyzes. In case all the information about the PEC and its control loop is known, analytical models can be derived [3]–[6], a review can be found in [7]. However, it is desirable to design dc microgrids with COTS converters in order to reduce the cost and time-to-market of the installations. In these cases, generally, the information available about the converters is very limited due to confidentiality issues.

The blackbox models are behavioral models that can be obtained from the response of the converters to specific perturbations injected to their terminals. Blackbox models have been proposed for ac microgrids [8]–[12], however in this paper the focus will be in dc-dc converters. The different blackbox modeling approaches can be classified in three categories according to the kind of responses that they are able to reproduce [13]:

- Linear structures
- Static nonlinear structures
- Dynamic nonlinear structures

In this paper, the different blackbox approaches to model dc-dc PECs are reviewed and their capabilities and limitations are highlighted using a boost converter. The integration of dynamic weighting functions to the polytopic model is proposed and its performance is compared with other blackbox modeling approaches. The rest of the paper is organized as follows: in Section II the different blackbox modeling structures for dc-dc PECs are reviewed. In Section III the proposed dynamic weighting functions are detailed. In Section IV the performance of the different blackbox models is compared using the boost converter as case study. Finally, in Section V the conclusions of the paper are exposed.

II. BLACKBOX MODELING OF DC-DC PECs

Blackbox models are used in case the information about the PECs is not available. In those cases, identification techniques can be applied to obtain the transfer functions that approximate the response of the system to a certain perturbation in time or frequency domain.

The most important part in the design of a blackbox model is the selection of the model structure, which entails a trade-off between complexity and capabilities.

A. LINEAR STRUCTURES

The most common blackbox linear structures used for PECs are the two-port models [14]. The two-port representation is very interesting from a system-level perspective, as different PECs can be easily interconnected creating the desired EPDS. These models represent the input-output small-signal dynamic behavior of the PECs, therefore they are very useful for dynamic interaction analyzes. The most common kind of structure is the inverse hybrid parameters (G-parameters) model, which represents a voltage-controlled PEC connected to a voltage source. The equivalent electrical circuit and the block diagram of the model are depicted in Fig. 3. This model can be represented as:

$$\begin{pmatrix} v_o \\ i_{in} \end{pmatrix} = \begin{pmatrix} G(s) & -Z(s) \\ Y(s) & H(s) \end{pmatrix} \begin{pmatrix} v_{in} \\ i_o \end{pmatrix}, \tag{1}$$

where v and i are voltage and current, the subscript o and in indicate output and input respectively. The physical meaning

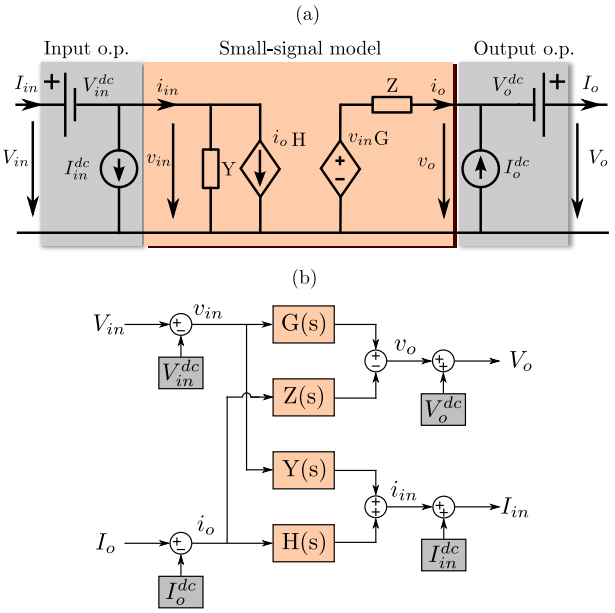

FIGURE 3. G-parameters model. (a) Equivalent electrical circuit, (b) Block diagram notation.

of the G-parameters is:

$$\begin{aligned} &\text{Audio-susceptibility} && \text{Input admittance} \\ &G(s) = \left.\frac{\tilde{v}_{out}}{\tilde{v}_{in}}\right|_{\tilde{i}_o=0} && Y(s) = \left.\frac{\tilde{i}_{in}}{\tilde{v}_{in}}\right|_{\tilde{i}_o=0} \\ &\text{Output impedance} && \text{Back current gain} \\ &Z(s) = \left.\frac{\tilde{v}_{out}}{\tilde{i}_o}\right|_{\tilde{v}_{in}=0} && H(s) = \left.\frac{\tilde{i}_{in}}{\tilde{i}_o}\right|_{\tilde{v}_{in}=0}. \end{aligned} \tag{2}$$

Notice that these models are linear because they are based on the superposition theorem, i.e. the output variables can be defined as the independent contribution of each of the input variables when the other inputs are set to zero. This method has been widely used for the analysis of supply and load interactions, as well as for system-level impedance-based stability assessment [15]–[21].

The methodology to identify the G-parameters of a converter working in a particular operating point can be found in [22], [23]. The approach involves the use of a voltage source and a controllable current load in order to set a fix operating point. Notice that in order to apply superposition, keeping a variable constant is equivalent to set its small-signal contribution to zero. Two tests are needed to obtain the four G-parameters (Fig. 4). In the first test, a perturbation is introduced in the load current, while keeping the input voltage constant, and the response of the output variables is measured. From this test the output impedance and the back current gain can be identified. The second test is analogous, introducing the perturbation in the input voltage in this case, while keeping the output current constant. From this test the audio-susceptibility and the input admittance can be identified.

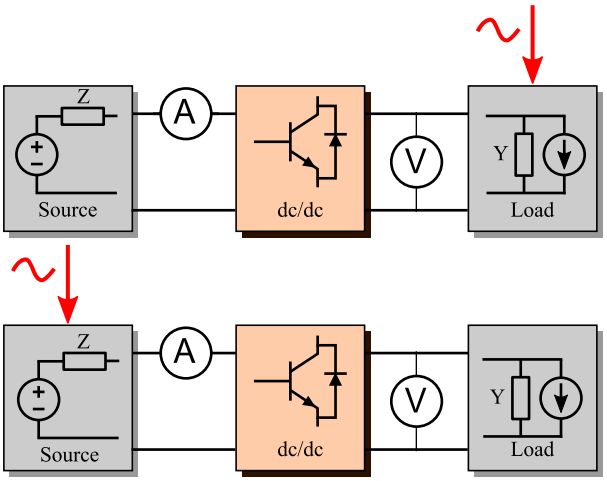

FIGURE 4. Test procedure to identify the G-parameters model. (a) Load perturbation, (b) Source perturbation.

In general, the output impedance of the sources and the input admittance of controllable loads are designed to be small, so they do not affect the rest of the system. However, it is possible that in some applications their effect is not negligible. In [23] the methodology to obtain unterminated models is presented, i.e. a model that is not affected by the impedances of the source and the load used to perform the tests. The approach is to determine the contribution of these impedances in the response of the system and remove them from the final model.

Blackbox G-parameters models have been applied to EPDS based on COTS converters [24]. It is also possible to identify the small-signal state-space representation of a converter around an operating point as in [25]. Considering the small-signal assumption, this kind of structure can represent with high accuracy the dynamic of PECs.

B. STATIC NONLINEAR STRUCTURES

In some cases, the dynamic of the PECs can be approximated by a linear structure, however the steady-state response shows strong nonlinearities due to saturations, the response of actuators and sensors, the control strategy, etc. In these cases, the Wiener-Hammerstein approach is very convenient. In general, this model is a block-based approach, where the input and output dynamic behavior is represented by linear networks and the nonlinearities in the static response are captured by means of nonlinear references.

In the literature, two different applications of this method for dc PECs have been proposed. One is based on the two-port models, where the dc operating point is changed by a nonlinear function of the operating point [26]. The second is a circuit oriented network, where the linear dynamic response is represented by networks, which consist of passive elements, and the nonlinear references are included as controlled voltage and current sources with a nonlinear function that depends on the operating point [27]. The latter approach is depicted

in Fig. 5. The input network accounts for the input filter, the output network represents the dynamic behavior of the output filter and the control loop, and the upper network takes into accout the audiosusceptibility. This general network is able to approximate the dynamic behavior of any converter with a second order response. It is also possible to extend it to higher order responses by incorporating other passive elements [28].

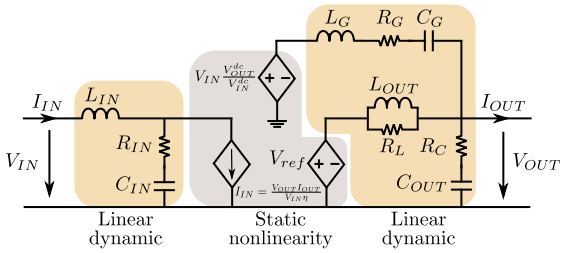

FIGURE 5. Oliver's Wiener-Hammerstein model.

One important difference between the two approaches is that in the former, the changes in the references affect directly the outputs of the model, whereas in the latter, the references are internal to the model, so they pass through the input and output filters before affecting the outputs of the model. Consequently, in the latter structure it is easy to implement protection systems, such as soft-start, over-under voltage protections, temperature protection, etc., [28].

C. DYNAMIC NONLINEAR STRUCTURES

In general, the response of the PECs is nonlinear. This nonlinearity can come from its switching nature, which makes the dynamic of the system dependent on the operating point; due to the nonlinear behavior of its internal components, magnetic elements and semiconductor devices; or due to its control strategy. From a blackbox perspective, the most common structure able to represent this kind of behavior is the polytopic model.

The politopic model consist of a collection of local models obtained around different operating points [29]. These small-signal models are integrated in a nonlinear structure by means of Weighting Functions (WF). The WFs have as inputs the input signals of the model and they control the local models which should contribute to the overall output of the polytopic model. The closer the current operating point to the operating point where the local model was obtained, the higher will be its weight. This idea is depicted in Fig. 6. The mathematical formulation of the model can be expressed as:

$$V_o = \sum_{i=1}^{n}\sum_{j=1}^{m} \omega_{ij}(\alpha, \beta, ...) V_{out}^{ij}(V_{in}, I_{out})$$
$$I_{in} = \sum_{i=1}^{n}\sum_{j=1}^{m} \omega_{ij}(\alpha, \beta, ...) I_{in}^{ij}(V_{in}, I_{out}) \quad (3)$$

where V_{out} and I_{in} are the output variables of the polytopic model, corresponding to the output voltage and the input

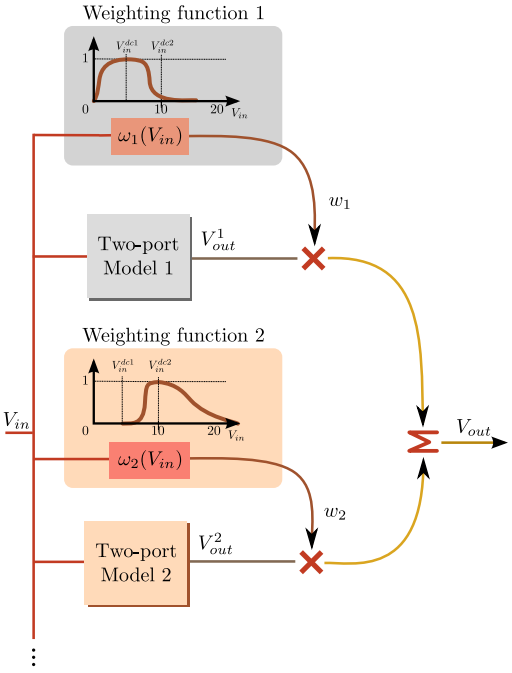

FIGURE 6. Polytopic model structure of a system with one input and one output variable.

current, ω_{ij} are the WF, and V_{out}^{ij} and I_{in}^{ij} are the output signals of the local model ij. Traditionally, the WF are static functions, and each of them is associated with each local model. They will have a value equal to 1 when the operating point of the model is equal to the one in which the local model was obtained, and it will decrease towards 0 as the operating point moves away from this point. These WFs must have values between 0 and 1 and the sum of all of them must be always equal to 1. These conditions can be expressed as:

$$0 \leq \omega_{ij}(\alpha, \beta, ...) \leq 1 \quad (4)$$
$$\sum_{i=1}^{n}\sum_{j=1}^{n} \omega_{ij}(\alpha, \beta, ...) = 1 \quad (5)$$

The most common shape of WF is the double sigmoid, which is a good compromise between a smooth transition among local models and simplicity in the mathematical expression. This function is defined by its center and slope. It is important that two adjacent local models have sigmoids with the same center and slope, so the condition (5) is complied with. The mathematical expression of the WF with a double sigmoid shape can be expressed as:

$$\omega_i(\alpha) = \left(\frac{1}{1+e^{-m_i(\alpha-c_i)}}\right) - \left(\frac{1}{1+e^{-m_{i+1}(\alpha-c_{i+1})}}\right) \quad (6)$$

where m_i and c_i are the slope and the center of the rising edge of the sigmoid and m_{i+1} and c_{i+1} are the slope and the center of the falling edge.

The polytopic model has also been used to model dc microgrids [30], [31], to design controllers [32] and to perform large-signal stability analyzes [33].

III. DYNAMIC WEIGHTING FUNCTIONS

The classical weighting functions are static, i.e. their outputs depend only on the current values of their inputs. However, it has been demonstrated that the changes in the dynamic behavior of a PEC has its own dynamic [34]. The dynamic behavior of a system can be expressed using the state-space representation. In particular, the state matrix is the one that characterizes the dynamic response of the system. One important characteristic of the state variables is that they cannot change instantly, because they are defined by their derivatives. However, in general, the relationship between the state variables and their derivatives can be nonlinear. A small-signal model around an equilibrium point can approximate this nonlinear relationship. Considering several equilibrium points, a piece-wise nonlinear model can be derived.

Generally, the state variables of a system are not known when using a blackbox approach. Hence, the inputs of the weighting functions are the inputs of the model, which do not have to be state variables. Usually, these input signals do not have constrains in their dynamic behavior, e.g. they could have a step-like variation. Consequently, using the traditional weighting functions, the model would change drastically its dynamic behavior from the one of the initial operating point to the one of the final operating point, which is defined by the input signal.

The idea of the dynamic weighting functions is to add a dynamic constraint to the variations in the dynamic response of the model. The goal is to approximate the dynamic behavior of the state variables from the perturbation in the input signals and to use this approximation as an input of the weighting functions. Mathematically, the response of the state variables can be related with the input signals as follows, consider a general state-space representation:

$$sx(s) = Ax(s) + Bu(s), \tag{7}$$

where $x(s)$ is the state vector, $u(s)$ is the input vector, A is the state matrix, and B is the input matrix. The transfer function between the state and the input vector is:

$$\frac{x(s)}{u(s)} = (sI - A)^{-1}B, \tag{8}$$

where I is the identity matrix. Equation (8) can be also expressed as:

$$\frac{x(s)}{u(s)} = \frac{1}{det(sI - A)} adj(sI - A)B, \tag{9}$$

where $adj()$ is the adjugate of a matrix and $det()$ is the determinant of a matrix. Notice that $det(sI - A)$ corresponds with the characteristic polynomial, which defines the poles of the system and they can be found in all the transfer functions, if they are observable. A possible conclusion of this analysis is that, in case the state variables are unknown, as it is the case when using blackbox models, the poles of the system are a good approximation for the dynamic behavior of the state variables.

Consequently, the dynamic weighting functions can be designed based on this information. First, the classical weighting functions are implemented such that the small-signal models have their maximum effect when the operating point is in the value in which they where obtained. Then, the characteristic filter, i.e. a transfer function made with the poles of the system, is inserted between the input signal and the static weighting functions. Therefore, the input of the static weighting functions has the steady-state value of the input and its dynamic is approximated to the dynamic of the state variables. Finally, the expression of the characteristic filter can be expressed as:

$$\tau(s) = \frac{a_0}{det(sI - A)} = \frac{a_0}{s^n + ... + a_1 s + a_0} \tag{10}$$

where $\tau(s)$ is the characteristic filter. The denominator would consist of a collection of the poles of the system. Notice that due to pole-zero cancellations, not all the poles must define the dynamic behavior of all the state variables. Finally, the numerator is designed such that in the steady-state the gain of the filter is unitary. The mathematical expression of a dynamic weighting function can be expressed as:

$$w(u(s), s) = w_s(u(s)\tau(s)), \tag{11}$$

where $w(u(s), s)$ is the dynamic weighting function and $w_s(u(s)\tau(s))$ is the static weighting function. The scheme of a one dimensional dynamic weighting function is depicted in Fig. 7.

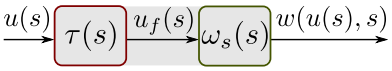

FIGURE 7. Scheme of a dynamic weighting function.

In nonlinear systems, the poles of the system can vary with the operating point, therefore the characteristic filter can also be designed such that it depends on the input variables.

IV. CASE STUDY: BOOST CONVERTER

In this section, the blackbox modeling approaches detailed in Section II will be applied to a boost converter in order to highlight their capabilities and limitations. The switching model of the boost converter will be used as test bench. This kind of model is able to capture the dynamic dependency of the PECs with the operating point and the problems related with noise and measurement equipment is avoided. Therefore, they are considered very useful to classify the models according to the kind of nonlinearities that they are able to reproduce. In particular, the analysis will be made using a voltage-controlled boost converter.

The voltage-controlled boost converter has been used because it is one of the simplest topologies that present a considerably strong operating point dependent behavior. In [13] the mathematical expression of the averaged dynamic behavior of the converter is detailed in open and closed loop, where operating point dependent dynamic behavior of

the converter is highlighted. Besides, the frequency response of the G-parameters linearized around different equilibrium points is depicted in order to represent graphically the variability in the dynamic behavior of the converter.

A. BOOST CONVERTER

1) COMPARISON OF THE DIFFERENT BLACKBOX MODELING STRUCTURES

Figure 8 shows the scheme of the voltage-controlled synchronous boost converter regulated with a PI controller.

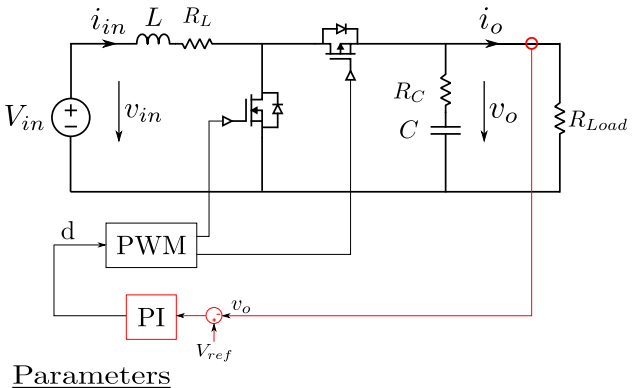

Parameters

$R_L = 0.1\Omega$ $\quad K_p = 0.01$
$L = 500\mu H$ $\quad K_i = 10$
$R_C = 0.01\Omega$ $\quad f_{PWM} = 100kHz$
$C = 62.5\mu F$

FIGURE 8. Voltage-controlled synchronous boost converter circuit.

The G-parameters models used in the comparison will be obtained around different operating points of the two inputs considered. In particular, the points selected are the nine combinations of $V_{in} = \{20, 22, 24\}$ V and $I_{out} = \{1, 5, 9\}$ A. As small-signal model, the G-parameters model obtained for $V_{in} = 24$ V and $I_{out} = 1$ A is used. The nine small-signal models are integrated in a polytopic structure, using the middle points between operating points as center of the weighting functions and a slope of 4 for both variables. The Wiener-Hammerstein model was obtained using identification techniques from the response of the converter to steps in the input voltage and the output current. The output filter of the Wiener-Hammerstein model shown in Fig. 5 is of second order and it was not able to reproduce the response of the converter correctly, therefore an extra inductor (L_{out2}) was included in series with the resistor in parallel with the output inductance (R_L). The parameters obtained in the identification are shown in Table 1.

Figure 9 shows the comparison between the switching model and the three models obtained. The initial operating point is the one selected for the small-signal G-parameters model, $V_{in} = 24$ V and $I_o = 1$ A. At time $t = 1$ ms the input voltage has a negative step to $V_{in} = 20$ V, where it can be seen that the G-parameters and the Wiener-Hammerstein models start losing accuracy, whereas the polytopic model is able to follow the dynamic behavior of the transition. In particular,

TABLE 1. Parameters of the Wiener-Hammerstein model of the voltage-controlled synchronous boost converter.

Output filter		Input filter		Audiosuscentibility	
L_{out}	$984.6\ \mu H$	L_{in}	$57.2\ \mu H$	L_G	$402.8\ \mu H$
R_L	$1.92\ \Omega$	R_{in}	$0.076\ \Omega$	R_G	$0.9\ \Omega$
C_{out}	$302.6\ \mu F$	C_{in}	$1.2\ mF$	C_G	$0.22\ F$
R_C	$8.7\ \mu\Omega$				
L_{out2}	$1.2\ mH$				

the mean error of the polytopic model in this transition has a 68.4% less error than the G-parameters model and a 62.4% less error than the Wiener-Hammerstein model for the output voltage. Regarding the input current the improvements are of 46.9% and 49.4%, respectively.

At time $t = 6$ ms a resistor is connected in parallel with the output, making the output current increase to $I_o = 9$ A. In this case the error of the G-parameters and Wiener-Hammerstein models becomes higher in the transient response. Besides, the G-parameters model starts to fail also in the steady-state of the input current, whereas the Wiener-Hammerstein model is able to track this value due to the nonlinear reference included in the input network (see Fig. 5). The polytopic model is more accurate, however some errors can be noticed at the beginning of the transition: in the output voltage the overshoot of the model is higher than the switching model; and in the input current there is an initial negative step. The reason for the initial negative step in the input current is that, due to the sharp step in the output current, the weighting functions change both sharply, changing abruptly the output of the model from the G-parameters model obtained in $V_{in} = 20$ V and $I_o = 1$ A (the operating point before the load step) to the one obtained for $V_{in} = 20$ V and $I_o = 9$ A. As this second model has static errors in the input current, the initial point of this variable is not at the same value. The relative error analysis shows a reduction of error of the polytopic model of 58.7% and 55.5% compared with the G-parameters and Wiener-Hammerstein models for the output voltage. Regarding the input current the improvement is 76.7% and 62.5% respectively.

Finally, at time $t = 11$ ms there is another step in the input voltage towards the initial value $V_{in} = 24$ V and the results are similar, the G-parameters and the Wiener-Hammerstein models do not capture accurately the dynamic behavior, whereas the polytopic model does it better, but with errors in the initial part of the transitory response. In this case the error in the steady-state value of the input current of the G-parameters model is lower than before because the operating point is closer to the value where it was obtained. The relative error improvement in this case is 45.8% and 40.6% for the output voltage and 57.2% and 49.2% for the input current.

In Fig. 10 different measures of the overall error of the models compared with the switching model are presented. It can be clearly seen that the polytopic model has the best

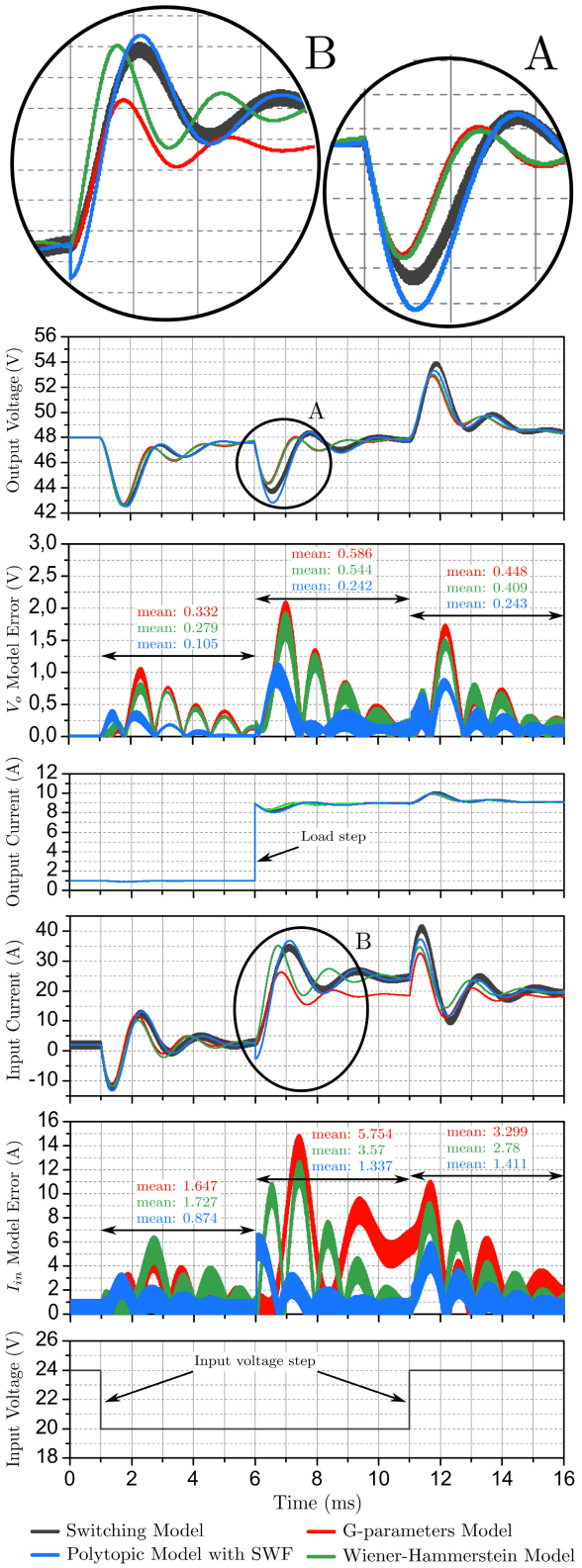

FIGURE 9. Comparison between the switching model and the three types of blackbox structures of a voltage-controlled synchronous boost converter.

performance both for the output voltage and the input current. The error reduction obtained using the polytopic model is around 50% for both variables.

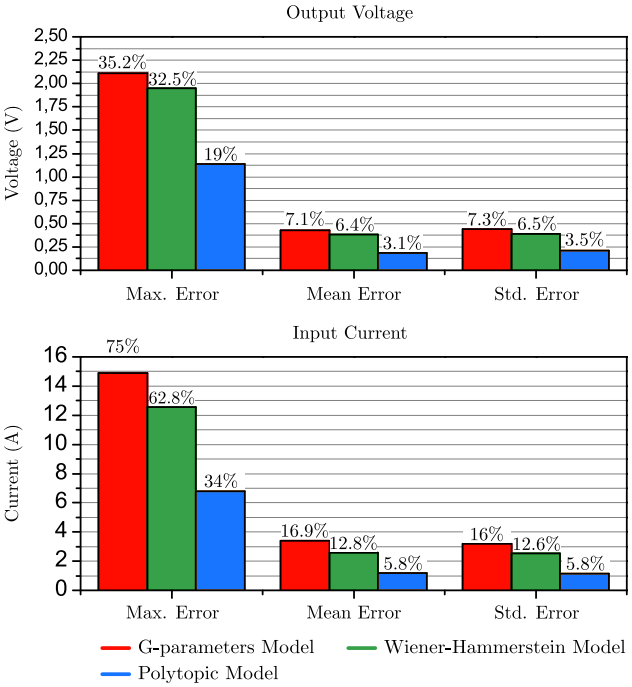

FIGURE 10. Error comparison between the switching model and the three types of blackbox structures of a voltage-controlled synchronous boost converter.

Regarding the simulation time, in this case the switching model takes 82 s to complete the simulation, whereas the G-parameters, Wiener-Hammerstein, and polytopic models take 2 s, 2 s, and 6 s, respectively. The main reason is that switching models need an integration time between 10 and 100 times smaller than the switching frequency in order to provide accurate results. On the other hand, the blackbox models are averaged models, therefore the integration time of the simulation can be greatly increased, as it does not consider the switching process. Consequently, as the switching frequency increases, the reduction in computational burden of the average models is more evident.

2) POLYTOPIC MODEL WITH DYNAMIC WEIGHTING FUNCTIONS

The previous section showed that the voltage-controlled synchronous boost converter has a variable dynamic behavior depending on its operating point. The G-parameters and the Wiener-Hammerstein models use linear models to account for the dynamic behavior of the converter, so they cannot account for this phenomenon. The polytopic model is able to adapt its dynamic response according to the operating point. However, it was shown that when a large step in the input variables occurs, the performance of the model at the initial part of the transitory was not accurate. In this section the use of dynamic weighting functions is introduced in order to approximate the rate of change in the dynamic behavior of the converter with the poles of the system. The operating points considered are again all possible combinations of $V_{in} = \{20, 22, 24\}$ and $I_o = \{1, 5, 9\}$.

The static part of the weighting functions is the same as in the polytopic model used in the previous section, i.e. the centers of the sigmoids are set in the middle of the operating points considered and the slope is 4 for the input voltage and the output current. The transfer function that provides dynamic to the weighting functions has been designed using (10). The poles of the initial operating point, $V_{in} = 20\ V$ and $I_o = 1\ A$, were selected and the resulting transfer function is:

$$\tau(s) = \frac{624.47e7}{s^3 + 2082.72s^2 + 116.67e5s + 624.47e7} \quad (12)$$

The same transfer function is used for both the input voltage and the output current.

In Fig. 11 the response of the switching model of the voltage-controlled boost converter to steps in the input voltage and in the load is compared with the polytopic models with static and dynamic weighting functions. At time $t = 1\ ms$ a step in the input voltage occurs, reducing its value from $V_{in} = 24\ V$ to $V_{in} = 20\ V$. The response of the polytopic model with static weighting functions is reasonably accurate, so only a modest improvement can be seen in the model using dynamic weighting functions. However, it is interesting to see the effect of using the dynamic weighting functions in the transition among small-signal models. The step in the input voltage is sharp, therefore the polytopic model with static weighting functions modifies instantly its dynamic behavior between the initial point, $V_{in} = 24\ V$ and $I_o = 1\ A$, to the final point, $V_{in} = 20\ V$ and $I_o = 1\ A$. On the other hand, the polytopic model with dynamic weighting functions filters the step in the input voltage (green line), hence the input to its static weighting functions is not sharp but has the dynamic imposed by the poles of the system. Consequently, the dynamic of the polytopic model with dynamic weighting functions makes a transition starting in the initial operating point, $V_{in} = 24\ V$ and $I_o = 1\ A$, then activating the dynamic of the next small-signal model towards the final operating point, $V_{in} = 22\ V$ and $I_o = 1\ A$, and ultimately the final operating point, $V_{in} = 20\ V$ and $I_o = 1\ A$.

At time $t = 6\ ms$ a resistor is connected in parallel with the load, increasing the output current sharply from $I_o = 1\ A$ to $I_o = 9\ A$. Similarly to the previous step, the polytopic model with static weighting functions makes a sharp transition from the initial operating point, $V_{in} = 20\ V$ and $I_o = 1\ A$, to the final one $V_{in} = 20\ V$ and $I_o = 9\ A$, whereas the dynamic weighting functions experience a transition from the initial operating point $V_{in} = 20\ V$ and $I_o = 1\ A$, the next operating point towards the final one, $V_{in} = 20\ V$ and $I_o = 5\ A$, and finally the last operating point, $V_{in} = 20\ V$ and $I_o = 9\ A$. Regarding the performance of the models, in this case a considerable improvement can be seen in the initial part of the transition. The estimation of the voltage drop due to the load step of the polytopic model with static weighting functions is around $5\ V$, whereas the actual value is $4\ V$ corresponding to a mismatch of 25%. Using the dynamic weighting functions the errors are contained to less than 5%. Concerning the input current, the initial operating point is $I_{in} = 2.5\ A$, however when the load step occurs the model with static weighting functions suddenly jumps to $I_{in} = -2.5\ A$ and then starts the transitory response towards the final value, $I_{in} = 25\ A$.

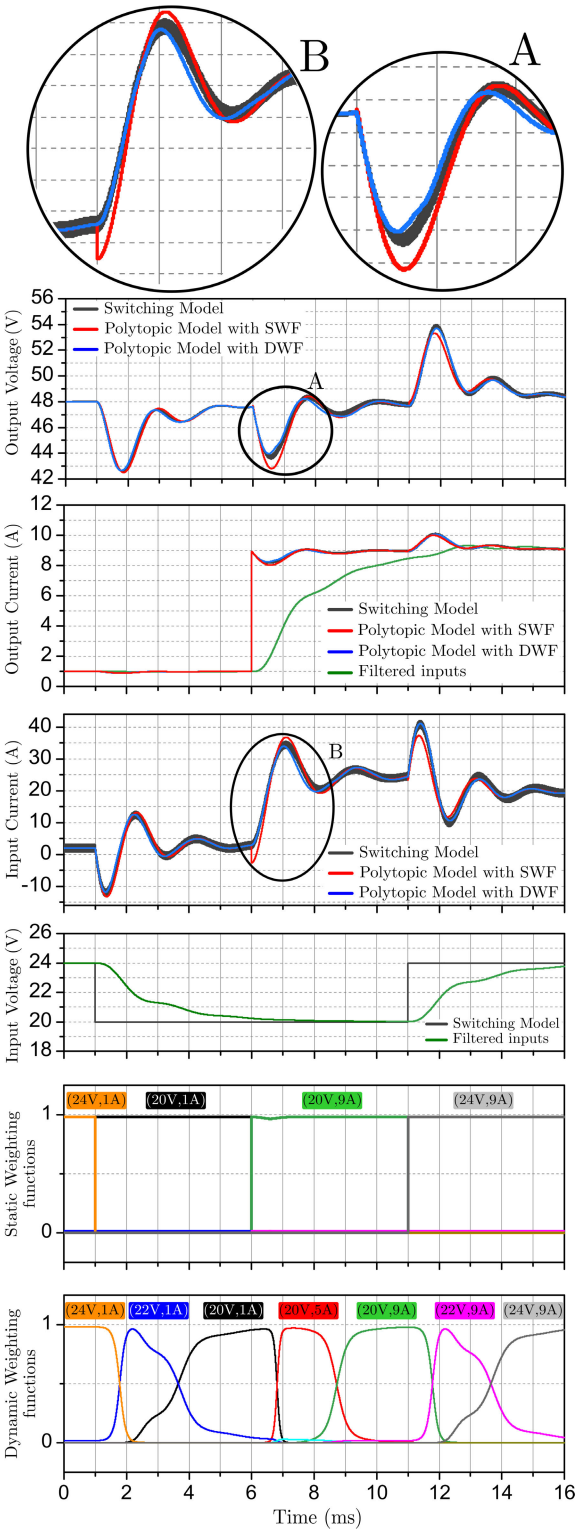

FIGURE 11. Comparison between the switching model and the polytopic model with the classical static weighting functions (SWF) and with the proposed dynamic weighting functions (DWF) for the case of a voltage-controlled boost converter.

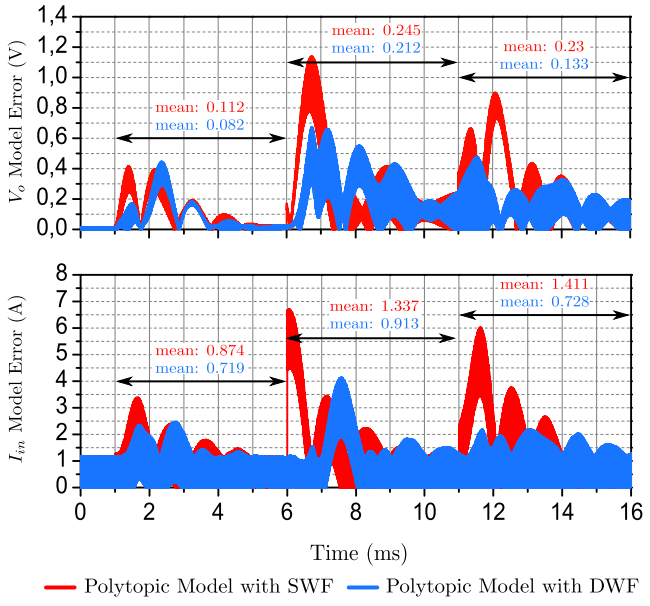

FIGURE 12. Error signals between the switching model and the polytopic model with the classical static weighting functions (SWF) and with the proposed dynamic weighting functions (DWF) for the case of a voltage-controlled boost converter.

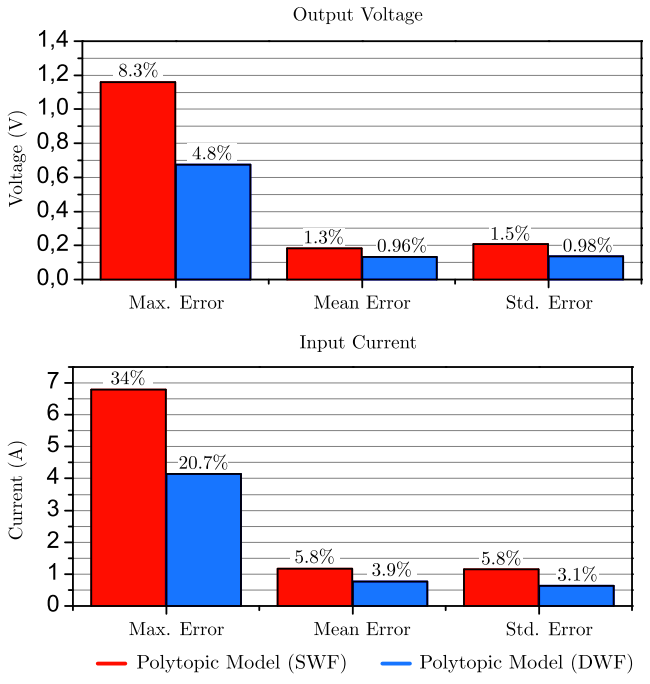

FIGURE 13. Details about the performance of the polytopic model with the classical static weighting functions (SWF) and with the proposed dynamic weighting functions (DWF) for the case of a voltage-controlled boost converter.

This undesired behavior is due to the nonlinearity in the dc gain of the back current gain, and the sharp transition among small-signal models. The small-signal model corresponding to the final operating point, $V_{in} = 20\ V$ and $I_o = 9\ A$, initially is at $-8\ A$ from its nominal value. As this model has a higher dc gain than the small-signal model corresponding to the initial point, $V_{in} = 20\ V$ and $I_o = 9\ A$, there is an error in the steady state value of the input current. As the polytopic model with static weighting functions change instantly to the final small-signal model, this error appears in the output of the model. Using the dynamic weighting functions, this change among small-signal models is gradual, therefore it starts from the correct dc value and reflects the transition with high accuracy.

Finally, at time $t = 11\ ms$ there is a step in the input voltage from $V_{in} = 20\ V$ to $V_{in} = 24\ V$. As in the previous cases, the sharp transition of the polytopic model with static weighting functions does not reflect the dynamic behavior accurately during the first part of the transitory, having a lower estimation of the overshoot of both the output voltage and the input current. On the other hand, the use of the dynamic weighting functions allows the model to make a transition among small-signal models, which is demonstrated to be an accurate approximation of the response of the actual behavior of the electric power converter to sharp and large steps in the input variables. The error between the switching model and the two blackbox models obtained is shown in Fig. 12 and Fig.13.

V. CONCLUSION

In this paper the concept of dynamic weighting function has been introduced. This method aims to approximate the dynamic of the state variables by filtering the input-output variables of the model with a transfer function designed from the information of the poles of the system. This transfer function has a unitary gain to avoid the distortion of the variables in the steady state. The rationale of this proposal is that the nonlinear behavior in power electronic converters can be due to nonlinearities related with the state variables, which are not available in blackbox models. By using what it has been named as the *characteristic filter*, the inputs to the traditional static weighting functions are not directly the input-output variables, which can change sharply, but these variables filtered by the mentioned *characteristic filter*. This causes that the transition among the small-signal models, which integrate the polytopic model, is not necessarily as sharp as the step in the input variables, but it is limited by the dynamic of the poles of the system, which is related with the dynamic of the state variables.

A voltage-controlled boost converter has been used as case study. After sharp steps in the input variables of the model, the polytopic model with dynamic weighting functions makes a transition through all the small-signal models between the initial and the final operating point, whereas the polytopic model with static weighting functions changes abruptly and directly to the final operating point. This limitation in the rate of change among small-signal models, that is, in the rate of change in the dynamic behavior of the PECs, has been proved to be a better approximation to the real behavior of switching converters. As future work, other kind of nonlinearities such as controllers with different operating modes and saturation of the duty cycle, will be considered.

REFERENCES

[1] D. Boroyevich, I. Cvetković, D. Dong, R. Burgos, F. Wang, and F. Lee, "Future electronic power distribution systems a contemplative view," in *Proc. 12th Int. Conf. Optim. Elect. Electron. Equip.*, May 2010, pp. 1369–1380.

[2] J. M. Guerrero, J. V. Vásquez, and R. Teodorescu, "Hierarchical control of droop-controlled DC and AC microgrids—A general approach towards standardization," in *Proc. 35th IEEE Annu. Conf. Ind. Electron. Soc.*, Nov. 2009, pp. 4305–4310.

[3] Z. M. Dalala, Z. U. Zahid, O. S. Saadeh, and J.-S. Lai, "Modeling and controller design of a bidirectional resonant converter battery charger," *IEEE Access*, vol. 6, pp. 23338–23350, 2018.

[4] A. Elserougi, I. Abdelsalam, A. Massoud, and S. Ahmed, "A non-isolated hybrid-modular DC-DC converter for DC grids: Small-signal modeling and control," *IEEE Access*, vol. 7, pp. 132459–132471, 2019.

[5] J. Luo, X.-P. Zhang, and Y. Xue, "Small signal model of modular multi-level matrix converter for fractional frequency transmission system," *IEEE Access*, vol. 7, pp. 110187–110196, 2019.

[6] L. Wang, X. Deng, P. Han, X. Qi, X. Wu, M. Li, and H. Xu, "Electromagnetic transient modeling and simulation of power converters based on a piecewise generalized state space averaging method," *IEEE Access*, vol. 7, pp. 12241–12251, 2019.

[7] A. Francés, R. Asensi, O. García, R. Prieto, and J. Uceda, "Modeling electronic power converters in smart DC microgrids—An overview," *IEEE Trans. Smart Grid*, vol. 9, no. 6, pp. 6274–6287, Nov. 2018.

[8] I. Cvetkovic, M. Jaksic, D. Boroyevich, P. Mattavelli, F. C. Lee, Z. Shen, S. Ahmed, and D. Dong, "Un-terminated, low-frequency terminal-behavioral d-q model of three-phase converters," in *Proc. IEEE Energy Convers. Congr. Expo.*, Sep. 2011, pp. 791–798.

[9] G. Guarderas, A. Frances, D. Ramirez, R. Asensi, and J. Uceda, "Black-box large-signal modeling of grid-connected DC-AC electronic power converters," *Energies*, vol. 12, no. 6, p. 989, 2019. [Online]. Available: https://www.mdpi.com/1996-1073/12/6/989

[10] V. Valdivia, A. Lazaro, A. Barrado, P. Zumel, C. Fernandez, and M. Sanz, "Black-box modeling of three-phase voltage source inverters for system-level analysis," *IEEE Trans. Ind. Electron.*, vol. 59, no. 9, pp. 3648–3662, Sep. 2012.

[11] Y. Shi, D. Xu, J. Su, N. Liu, H. Yu, and H. Xu, "Black-box behavioral modeling of voltage and frequency response characteristic for islanded microgrid," *Energies*, vol. 12, no. 11, p. 2049, 2019.

[12] H. Gong, D. Yang, and X. Wang, "Identification of the DQ impedance model for three-phase power converter considering the coupling effect of the grid impedance," in *Proc. IEEE Appl. Power Electron. Conf. Expo. (APEC)*, Mar. 2019, pp. 120–126.

[13] A. F. Roger, "Blackbox nonlinear modeling and stability analysis of DC electronic power converters in microgrids," Ph.D. dissertation, ETSI Ind. (UPM), Madrid, Spain, 2018.

[14] P. G. Maranesi, V. Tavazzi, and V. Varoli, "Two-part characterization of PWM voltage regulators at low frequencies," *IEEE Trans. Ind. Electron.*, vol. 35, no. 3, pp. 444–450, Aug. 1988.

[15] B. H. Cho and F. C. Y. Lee, "Modeling and analysis of spacecraft power systems," *IEEE Trans. Power Electron.*, vol. 3, no. 1, pp. 44–54, Jan. 1988.

[16] T. Suntio, M. Hankaniemi, and M. Karppanen, "Analysing the dynamics of regulated converters," *IEE Proc.—Electr. Power Appl.*, vol. 153, no. 6, pp. 905–910, Nov. 2006.

[17] M. Hankaniemi, M. Karppanen, T. Suntio, A. Altowati, and K. Zenger, "Source-reflected load interactions in a regulated converter," in *Proc. 32nd Annu. Conf. IEEE Ind. Electron.*, Nov. 2006, pp. 2893–2898.

[18] M. Veerachary and A. R. Saxena, "G-parameter based stability analysis of DC-DC power electronic system," in *Proc. IEEE Joint Int. Conf. Power Syst. Technol. Power India Conf.*, Oct. 2008, pp. 1–4.

[19] J. Leppäaho, J. Huusari, L. Nousiainen, and T. Suntio, "Dynamics of current-fed converters and stability-assessment of solar-generator interfacing," in *Proc. IEEE Int. Power Electron. Conf.*, Jun. 2010, pp. 703–709.

[20] S. Vesti, T. Suntio, J. A. Oliver, R. Prieto, and J. A. Cobos, "Impedance-based stability and transient-performance assessment applying maximum peak criteria," *IEEE Trans. Power Electron.*, vol. 28, no. 5, pp. 2099–2104, May 2013.

[21] S. Padhee, U. C. Pati, and K. Mahapatra, "Closed-loop parametric identification of DC-DC converter," *Proc. Inst. Mech. Eng., I, J. Syst. Control Eng.*, vol. 232, no. 10, pp. 1429–1438, 2018.

[22] L. Arnedo, D. Boroyevich, R. Burgos, and F. Wang, "Un-terminated frequency response measurements and model order reduction for black-box terminal characterization models," in *Proc. 23rd Annu. IEEE Appl. Power Electron. Conf. Expo.*, Feb. 2008, pp. 1054–1060.

[23] I. Cvetkovic, D. Boroyevich, P. Mattavelli, F. C. Lee, and D. Dong, "Un-terminated, low-frequency terminal behavioral model of DC-DC converters," in *Proc. 26th Annu. IEEE Appl. Power Electron. Conf. Expo. (APEC)*, Mar. 2011, pp. 1873–1880.

[24] S. Vesti, J. A. Oliver, R. Prieto, J. A. Cobos, and T. Suntio, "Stability and transient performance assessment in a cots-module-based distributed DC/DC system," in *Proc. IEEE 33rd Int. Telecommun. Energy Conf. (INTELEC)*, Oct. 2011, pp. 1–7.

[25] G. Herbst, "A building-block approach to state-space modeling of DC-DC converter systems," *J. Multidisciplinary Sci. J.*, vol. 2, no. 3, pp. 247–267, 2019.

[26] I. Cvetkovic, D. Boroyevich, P. Mattavelli, F. C. Lee, and D. Dong, "Non-linear, hybrid terminal behavioral modeling of a DC-based nanogrid system," in *Proc. 26th Annu. IEEE Appl. Power Electron. Conf. Expo. (APEC)*, Mar. 2011, pp. 1251–1258.

[27] J. A. Oliver, R. Prieto, J. A. Cobos, O. Garcia, and P. Alou, "Hybrid Wiener-Hammerstein structure for grey-box modeling of DC-DC converters," in *Proc. Appl. Power Electron. Conf. Expo.*, Feb. 2009, pp. 280–285.

[28] J. A. O. Ramírez, "Modelado comportamental de convertidores CC-CC para el análisis y simulación de sistemas distribuidos de potencia," Ph.D. dissertation, ETSI Ind. (UPM), Madrid, Spain, 2007.

[29] L. Arnedo, D. Boroyevich, R. Burgos, and F. Wang, "Polytopic black-box modeling of DC-DC converters," in *Proc. IEEE Power Electron. Spec. Conf.*, Jun. 2008, pp. 1015–1021.

[30] A. Francés, R. Asensi, O. García, R. Prieto, and J. Uceda, "A black-box modeling approach for DC nanogrids," in *Proc. Appl. Power Electron. Conf. Expo.*, Mar. 2016, pp. 1624–1631.

[31] A. Francés, R. Asensi, O. García, R. Prieto, and J. Uceda, "The performance of polytopic models in smart DC microgrids," in *Proc. IEEE Energy Convers. Congr. Expo. (ECCE)*, Sep. 2016, pp. 1–8.

[32] M.-A. Rodríguez-Licea, F.-J. Perez-Pinal, A.-I. Barranco-Gutiérrez, and J.-C. Nuñez-Perez, "Switched polytopic controller applied on a positive reconfigurable power electronic converter," *Energies*, vol. 11, no. 1, p. 116, 2018.

[33] A. Francés, R. Asensi, O. García, and J. Uceda, "A blackbox large signal Lyapunov-based stability analysis method for power converter-based systems," in *Proc. IEEE 17th Workshop Control Modeling Power Electron. (COMPEL)*, Jun. 2016, pp. 1–6.

[34] A. Francés, R. Asensi, O. García, and J. Uceda, "How to model a DC microgrid: Towards an automated solution," in *Proc. IEEE 2nd Int. Conf. DC Microgrids (ICDCM)*, Jun. 2017, pp. 609–616.

AIRÁN FRANCÉS (GS'16–M'18) received the M.Sc. and Ph.D. degrees in electrical engineering from the Universidad Politécnica de Madrid (UPM), Spain, in 2012 and 2018, respectively.

He is currently an Assistant Professor with the Department of Electrical Engineering, UPM. He participated for two years in the European Project XFEL, where he collaborated in the design and development of dc–dc power supplies for superconducting magnets. His current research interests include modeling, control and stability assessment of electronic power distribution systems, and smart grids.

RAFAEL ASENSI was born in Madrid, Spain, in 1966. He received the M.Sc. and Ph.D. degrees in electrical engineering from the Universidad Politécnica de Madrid (UPM), Madrid, Spain, in 1991 and 1998, respectively.

He joined the Department of Electrical Engineering, in 1994, where he is currently an Associate Professor. His research interest includes high-frequency modeling of magnetic components and nonlinear load modeling and simulation.

JAVIER UCEDA (M'83–SM'91–F'05) received the M.Sc. and Ph.D. degrees in electrical engineering from the Universidad Politécnica de Madrid (UPM), Spain, in 1976 and 1979, respectively.

He is currently a Full Professor in electronics with the Electrical and Electronic Engineering Department, UPM. His research activity has been developed in the field of power electronics, where he has participated in numerous national and international research projects. His research interests include switched-mode power supplies and dc–dc power converters for telecom and aerospace applications. As a result of this activity he has published more than three hundred articles in international journals and conferences. He holds several national and international patents.

Prof. Uceda has received several individual and collective awards, such as the IEEE Third Millennium Medal, the Puig Adán Medal. He is also a Honorary Doctor by the Universidad Ricardo Palma in Perú and the Colegio de Posgraduados in Mexico.